Chemical Geology 272 (2010) 12–19

Contents lists available at ScienceDirect

Chemical Geology

journal homepage: www.elsevier.com/locate/chemgeo

Platinum element group variations at the Permo–Triassic boundary in Kashmir and British Columbia and their significance

M.E. Brookfield [a,*], J.G. Shellnutt [a], Liang Qi [b], R. Hannigan [c], G.M. Bhat [d], P.B. Wignall [e]

[a] Institute of Earth Sciences, Academia Sinica, Nankang, Taipei 11529, Taiwan
[b] Institute of Geochemistry, Chinese Academy of Sciences, Guiyang 550002, China
[c] Department of Environmental, Earth and Ocean Sciences, University of Massachusetts at Boston, 100 Morrissey Boulevard, Boston, MA 02125, USA
[d] Postgraduate Department of Geology, University of Jammu, J&K State, India
[e] School of Earth and Environment, University of Leeds, Leeds LS2 9JT, UK

ARTICLE INFO

Article history:
Received 6 May 2009
Received in revised form 13 January 2010
Accepted 16 January 2010

Editor: J.D. Blum

Keywords:
Group
Permo–Triassic
Boundary
Kashmir
British Columbia

ABSTRACT

The end Permian marks the greatest extinction in the geological record, but there is no consensus on whether it was caused by terrestrial or extraterrestrial factors. Platinum group elements (PGE) can readily separate extraterrestrial from terrestrial sources and the few studies so far (from China and Europe) indicate terrestrial sources for the PGE. We report here detailed PGE analyses of two expanded sections from the late Permian northern and southern hemispheres that allow separate events to be distinguished and confirm a terrestrial source for the PGE. These sources are either contemporaneous seawater or older basaltic volcanics associated with the sections and the PGE were precipitated by a possible combination of development of anoxia in the oceans and post-depositional redistribution. The PGE content in sections at the Permo–Triassic boundary is the result of geochemical and lithological control on metal precipitation that is found in many other black shales throughout geological time.

1. Introduction

The greatest extinction in the geological record took place at the end of the Permian around 251.5 Ma, killing over 90% of all marine and about 70% of all terrestrial species (Erwin, 2005). Both gradual environmental and catastrophic events have been used to explain the extinction but so far with little consensus. One problem is that relatively few rock sections are stratigraphically continuous across the boundary, and there are even fewer in which relatively thick sections allow individual late Permian events to be separated. For example, the Global Stratotype Section and Point (GSSP) for the Permian–Triassic boundary are defined at Meishan in South China (Yin et al., 2001) (Fig. 1) but the section is condensed compared to some others. The change of rock type (limestone to marl) and biostratigraphic boundary at Meishan are separated by less than 0.3 m (Yin et al., 2001). Within this 0.3 m interval at Meishan there are: a marked negative shift of stable carbon and sulfur isotopes (Kaiho et al., 2006) which can be used to define the interval elsewhere; a horizon of disputably increased iridium (up to 2.0 ppb in Xu and Yan, 1993), higher concentrations of some heavier elements like nickel and iron (Kaiho et al., 2006), and terrestrial-type platinum group element (PGE) concentrations (Xu et al., 2007). In other sections, like the Kashmir and British Columbia sections studied here, the two horizons are separated by thicker sedimentary units (Fig. 2) which allow distinct events to be better separated than at Meishan. The paleontology, stratigraphy, and some isotopic characteristics of these two expanded sections are reasonably well-known (e.g. Nakazawa et al., 1975; Wang et al., 1994; Henderson and Mei, 2000; Brookfield et al., 2003; Wignall and Newton, 2003; Wignall et al., 2005; Algeo et al., 2007) but little has been published on their geochemistry: and they have never been analyzed for PGE before.

PGE and their ratios in sediments can separate terrestrial from extraterrestrial sources. In this paper we wish to report variations in PGE in the widely separated sections in Kashmir and British Columbia, far from Meishan, and evaluate their significance.

2. Kashmir and British Columbia sections

Measurements in both sections are from the major lithological boundary just below the paleontologically defined Permo–Triassic

* Corresponding author.
E-mail address: mbrookfi@hotmail.com (M.E. Brookfield).

0009-2541/$ – see front matter © 2010 Elsevier B.V. All rights reserved.
doi:10.1016/j.chemgeo.2010.01.008

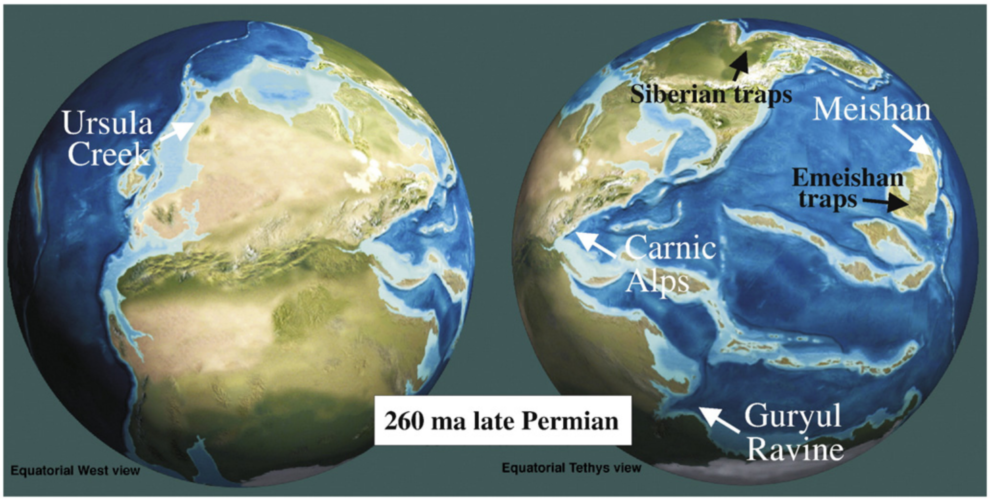

Fig. 1. Late Permian (260 ma) palaeogeography (courtesy Ron Blakey) with cited localities. Guryul is in central Kashmir State, India; Ursula Creek is in central British Columbia, Canada.

boundary, which is easily identified in both sections and is interpreted to mark a major environmental change (Algeo et al., 2007). Both sections formed part of their respective Permian continental margins and have not been significantly displaced relative to these margins since deposition: they are thus at or close to their Permian paleogeographic positions on the reconstruction (Fig. 1).

In Kashmir, India, the Permian–Triassic boundary sections have long been famous as among the most complete in the world, with apparent continuous sedimentation and gradual faunal changes across the boundary (Sheng et al., 1984). During the late Paleozoic, Kashmir formed part of Gondwana and lay on the southern side of the Paleotethys Ocean adjacent to Oman (Fig. 1). Rifting and eruption of middle Permian basalts (Guadalupian) were followed by separation of blocks off the northern edge of Gondwana, the formation of a Neotethys Ocean and rapid thermal subsidence of the northern Gondwana margin in the Upper Permian and Triassic (Brookfield, 1993). The well-known locality at Guryul Ravine, like Meishan, shows continuous, well-exposed sections across the Permian–Triassic boundary (Fig. 2), and was a candidate for the Global Stratotype Section and Point for the Permian–Triassic boundary (Yin et al., 2001). Paleoenvironmental analysis indicates that the upper Permian Zewan sandy limestones were laid down in a deep shelf environment subject to storm reworking (Brookfield et al., 2003). The topmost Zewan limestone shows much more intense wave reworking and may have been deposited either by successive large storm waves or by tsunami waves. If deposited at a depth of 100 m or greater (which is consistent

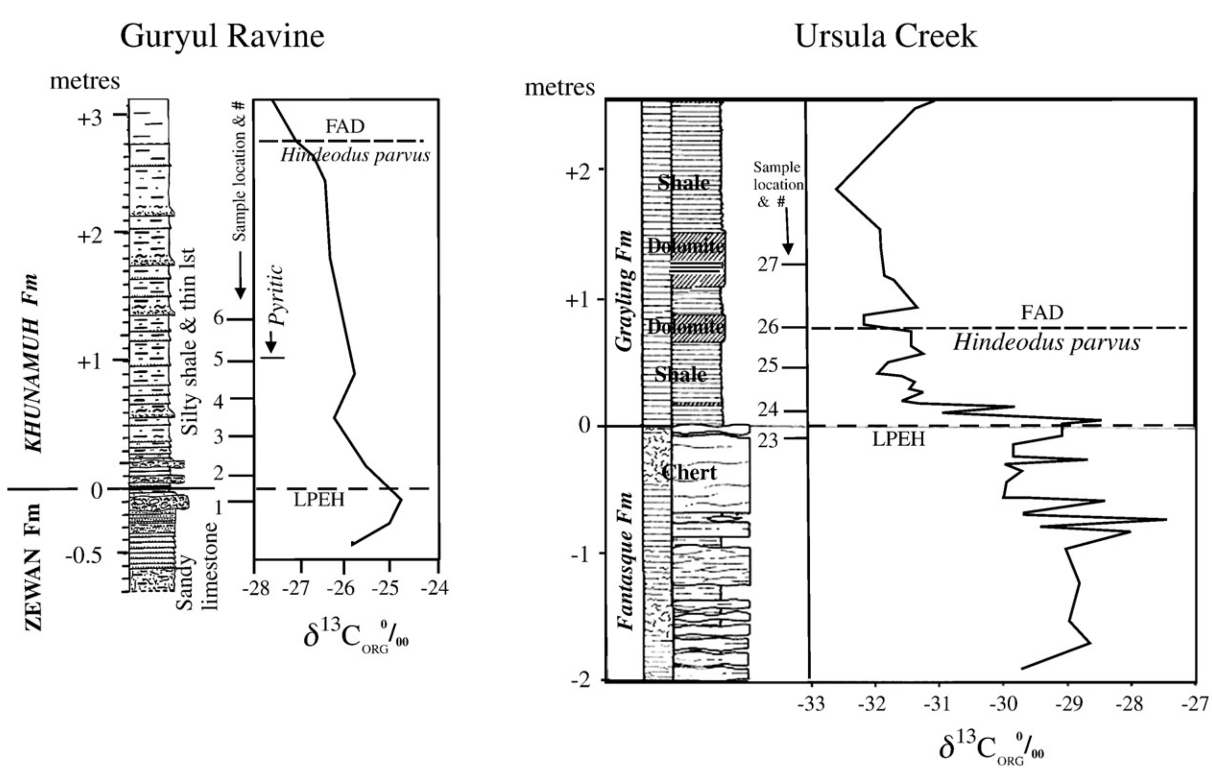

Fig. 2. Sections at Guryul Ravine and Ursula Creek with $\delta^{13}C$ organic trends, LPEH — Late Permian Event Horizon marked by major lithological change, and FAD — First Appearance Datum of the conodont *Hindeodus parvus* marking the base of the Triassic, and location of analyzed samples (from Wignall and Newton, 2003; Algeo et al., 2007).

Table 1
Blank (ng/g), detection limits (DL) (ng/g) and analytical results (ng/g) of PGE for reference materials, WGB-1 and WPR-1 (IUPAC, 1991; Govindaraju, 1994; Meisel and Moser, 2004; Qi and Zhou, 2008).

Elements	Blank	DL (3σ)	WGB-1 (Gabbro)			WPR-1 (Peridotite)	
			Average N = 6	Meisel	Certified	Average N = 6	Certified
Os	0.0026	0.0004	0.37 ± 0.02	0.544		14.5 ± 0.5	13
Ir	0.025	0.001	0.16 ± 0.02	0.211	0.33	13.8 ± 1.2	13.5
Ru	0.017	0.001	0.13 ± 0.01	0.144	0.3	23.1 ± 1.9	22
Rh	0.026	0.001	0.20 ± 0.02	0.234	0.32	12.8 ± 0.7	13.4
Pt	0.18	0.009	6.34 ± 0.61	6.39	6.1	280 ± 13	285
Pd	0.37	0.015	13.0 ± 1.1	13.9	13.9	238 ± 17	235

with the sedimentology), the bottom velocities required to move the coarse sand to cobble clasts in the bed indicate open-ocean waves of minimum size between 3 m amplitude/1000 s period and 40 m amplitude/10 s period (Brookfield et al., 2006, fig. 15). This bed is sharply overlain by the quieter water claystones and thin bioclastic limestones of the Khunamuh Formation. The fossil defining the base of the Triassic, *Hindeodus parvus*, first appears 2.7 m above the base of the Khunamuh Formation (from current studies) and anoxia, as determined by populations of small pyrite framboids, first appears at 1 m above the base (Wignall et al., 2005). The lower 1 m of the Khunamuh Formation is dominated by non-pyritic grey mudstone but also contains lenses and beds of shell material of late Permian aspect (Nakazawa et al., 1975; Brookfield et al., 2003). In 2007, we collected samples at 30 cm intervals across the boundary for geochemical analysis with the aim of simply characterizing any geochemical changes. Preliminary analysis with ICP-MS indicated high trace metal (including PGE) values in the basal 1 m of the lowermost Khunamuh Formation. The crucial samples in the lowermost Khunamuh Formation were therefore re-analyzed for PGE with isotope dilution inductively coupled plasma mass spectrometry (ID-ICP-MS) and nickel sulfide (NiS) fire assay combined with Te coprecipitation (Xu et al., 2007).

In British Columbia, the Ursula Creek section lies on the Permian deep continental slope margin of western North America (Jones, 1990). Here, as elsewhere in western and arctic Canada, the latest Permian event is marked by a lithological shift from cherty rocks to black shales and fine dolomites (Fig. 2) (Murchey and Jones, 1992). The first appearance of *Hindeodus parvus* at +0.75 m above the boundary (Wignall and Newton, 2003) suggests that Ursula Creek is more condensed than Guryul Ravine with 0 to +2.7 m at Guryul being temporally equivalent to 0 to +0.75 m at Ursula Creek and this also fits the $\delta^{13}C_{org}$ patterns where the minimum is higher than +3 m at Guryul but at +2 m at Ursula Creek (Fig. 2). As at Guryul, preliminary analysis showed somewhat elevated PGE values in the lowermost Triassic horizons of the basal Grayling Formation (though much less than at Guryul), so these horizons were also re-analyzed for PGE with ID-CP-MS and NiS fire assay.

3. Samples and methods

With the exception of sample GU-1 which is a moderately sorted bioclastic (dominantly brachiopod) limestone, all Guryul samples analyzed are dark grey (N3) to grayish black (N2) non-calcareous mudstones (Brookfield et al., 2003). At present, fairly large samples of the horizons so far collected from −70 m to +20 m in the Guryul Ravine section (at 0.3 m intervals from −0.1 m upwards) are housed at the Postgraduate Department of Geology of Jammu University, India, and splits are available to any workers who may wish to reanalyze the samples (please contact G.M. Bhat). The Ursula Creek samples are grey shale and one fine-grained dolomite (Wignall and Newton, 2003).

For the PGE analyses, the procedure for sample digestion and preconcentration is same as described by (Qi et al., 2007) using an improved Carius tube technique. Five grams of sample and appropriate amount of enriched isotope spike solution containing ^{193}Ir, ^{101}Ru, ^{194}Pt, ^{105}Pd and ^{190}Os were digested with 20 ml aqua regia in a 75 ml Carius tube placed in a custom-made, high pressure, water-filled, sealed autoclave. No Os or Ru was lost during aqua regia dry down (Qi et al., 2007). The internal pressure of the Carius tube is balanced by the external pressure produced by the water when heated to 300 °C to prevent explosion of the tube. After 10 h digestion, the Carius tube was cooled and the contents were transferred to a 50 ml centrifuge tube. After centrifuging, the upper solution was transferred to a distillation system for Os distillation and measurement by isotope dilution (ID-ICP-MS) and the residual solution was used for preconcentrating PGE by Te coprecipitation (Qi et al., 2004). All the interference elements, including Cu, Ni, Zr and Hf, were removed by using a cation exchange resin and P507 extraction chromatography resin combined in the same column (Qi et al., 2004). Samples were measured by ELAN DRC-e ICP-MS at the State Key Laboratory of Ore Deposit Geochemistry, Institute of Geochemistry, Chinese Academy of Sciences, Guiyang. Platinum, Pd, Ru, Os and Ir were measured by isotope dilution, whilst ^{194}Pt was used as the internal standard to calculate the concentration of the mono-isotope element Rh (Qi et al., 2004). The results of total procedural blanks and reference materials, WGB-1 (gabbro) and WPR-1 (peridotite) are listed in Table 1. The results of WPR-1 are in good agreement with the certified values. The results of Ru, Rh, and Ir for WGB-1 are lower than the certified values, but agree well with values reported by Meisel and Moser, (2004).

For other trace element analysis, the methods outlined in Algeo et al. (2007) were used. Since almost all the samples are non-calcareous argillites, corrections to carbonate-free analyses were only needed for GU −0.1 (a bioclastic grainstone) and UC 26 (a dolomitic mudstone) which contain less than 20% detrital minerals.

4. Results

PGE and selected metallic trace element results for the Guryul and Ursula Creek sections are shown on Table 2. Carbonate-free values are

Table 2
PGE and Au for Guryul and Ursula Creek. Upper continental crust values from Rudnik and Gao (2005, Table 3).

	Guryul						Ursula Creek				Upper continental crust
	−0.1	0.1	0.4	0.7	1	1.3	UC-23	UC-24	UC-26	UC-27	
Os (ng/g)	0.020	0.016	0.014	0.014	0.015	0.015	0.026	0.059	0.020	0.0082	0.031
Ir (ng/g)	0.033	0.021	0.026	0.030	0.033	0.025	0.003	0.042	0.030	0.027	0.022
Ru (ng/g)	0.060	0.055	0.051	0.056	0.057	0.048	0.026	0.043	0.060	0.083	0.34
Rh (ng/g)	0.033	0.025	0.028	0.027	0.025	0.024	0.015	0.036	0.030	0.064	–
Pt (ng/g)	0.50	0.339	0.456	0.471	0.454	0.501	1.787	0.723	0.37	0.855	0.5
Pd (ng/g)	0.380	0.734	2.796	4.070	4.389	0.809	0.488	0.735	0.64	1.125	0.52
Au (ng/g)	1.90	1.748	1.069	2.661	0.677	0.273	1.114	0.910	2.02	2.255	1.5
Pd/Pt	0.75	2.2	6.13	8.64	9.67	1.62	0.27	1.02	1.72	1.32	1.04
Ir/Pt	0.07	0.06	0.06	0.06	0.07	0.05	0.002	0.06	0.08	0.03	0.04
Ru/Rh	0.52	0.45	0.55	0.48	0.44	0.5	1.7	1.2	2.3	1.3	–
Os/Ir	0.6	0.8	0.5	0.5	0.45	0.6	8.7	1.4	0.8	0.3	1.44

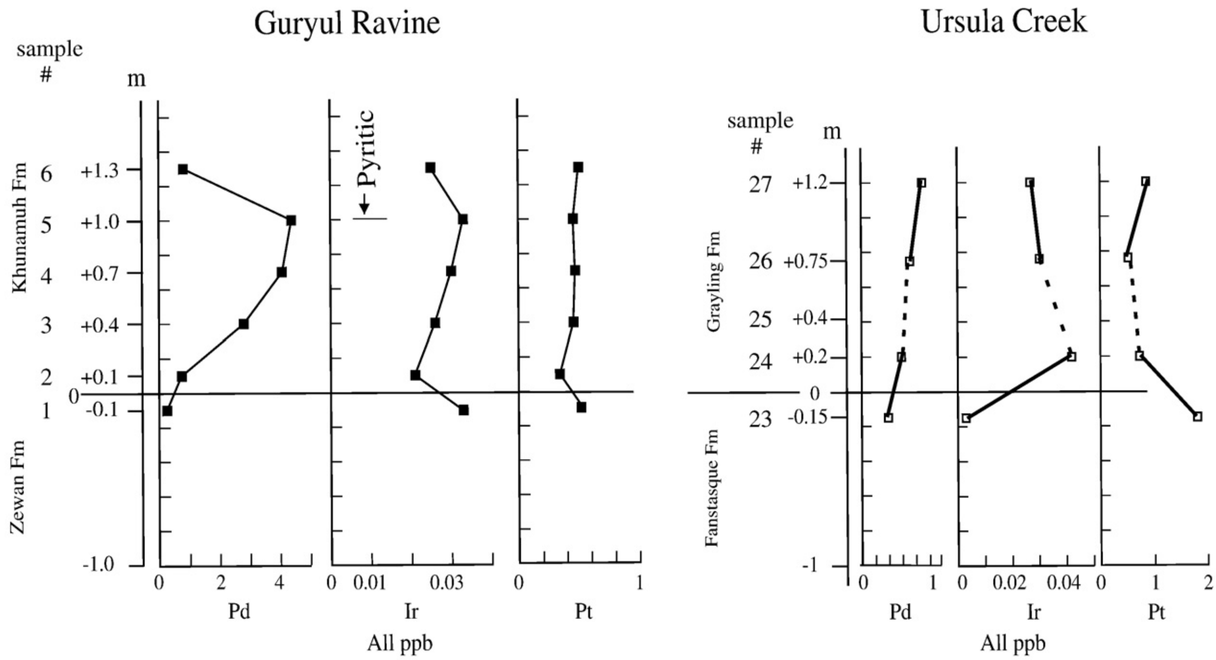

Fig. 3. Carbonate-free palladium, iridium and platinum variations in Guryul and Ursula Creek. Sample 25 from Ursula Creek was lost before analysis.

plotted on Figs. 3 and 4. These analyses show little variation in PGE around low mean values, apart from Pd at Guryul and Ir at Ursula Creek and none are much different from average values for Upper Continental Crust (Table 2). The metallic trace elements Ni, Cu, and Zn show somewhat greater variation around mean values in the lowermost Khunamuh Formation and, to a lesser extent, in the lowermost Grayling Formation below the paleontologically defined base of the Triassic at +2.7 m at Guryul and +0.75 m at Ursula Creek (Fig. 4). The total abundance of all PGE is, however, quite low (<6 ppb). The Guryul section has highest concentrations of Pd (0.38–4.39 ppb) and Au (0.27–2.66 ppb) however the Ursula Creek section has higher Pt (0.37–1.79 ppb). The remaining elements (Rh, Ru, Ir, and Os) from both sections have very low concentrations (<0.1 ppb each). The chondrite normalized PGE profiles show depleted iridium group (I–PGE) (Os, Ir, and Ru) patterns ($Ir/Pd_{Guryul} = 0.05–0.07$; $Ir/Pd_{Ursula\ Creek} = 0.02–0.08$), more depleted than Meishan and the Emeishan and Siberian basalts (Table 2, Fig. 5).

The chemostratigraphic profile of Guryul shows an increase of Pd from just below the Khunamuh Formation until the +1.0 m mark above which the concentrations decrease, Ir decreases then increases to a maximum at the +1.0 m mark though the differences are small; whereas Pt remains almost constant (Fig. 3). The +1.0 m mark corresponds to the main extinction event (extinction 1 of Algeo et al., 2007) and the first appearance of abundant pyrite framboids, which is used to determine the onset of anoxia (Wignall et al., 2005). Different trends are seen at Ursula Creek where Pd gradually increases slightly, Ir initially increases before decreasing (though the loss of sample 25 before PGE analysis makes this less certain). Platinum on the other

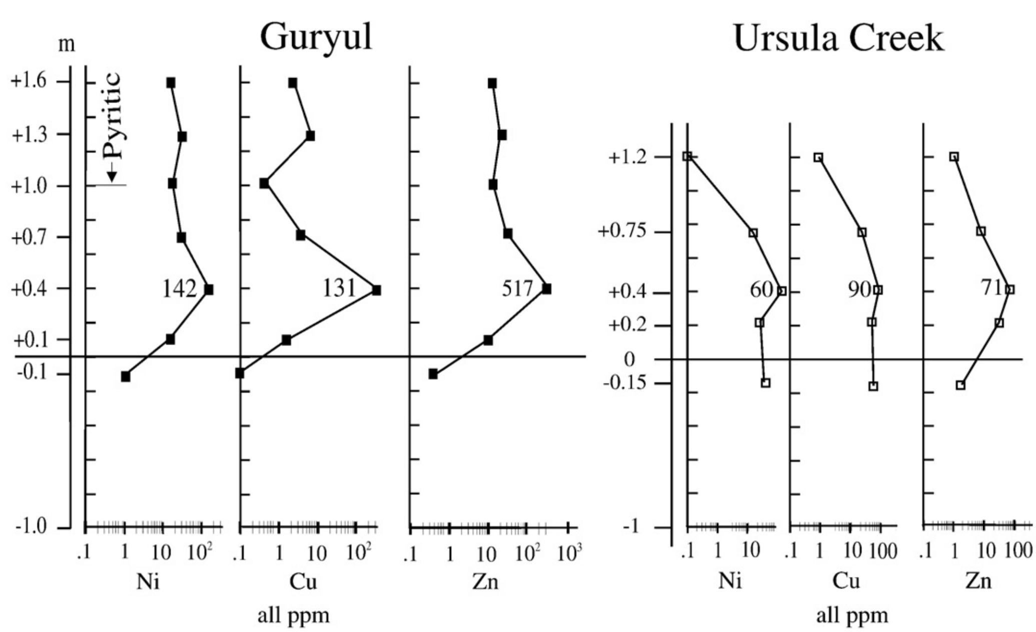

Fig. 4. Carbonate-free trace elements plots (Ni, Cu, Zn) for Guryul and Ursula Creek.

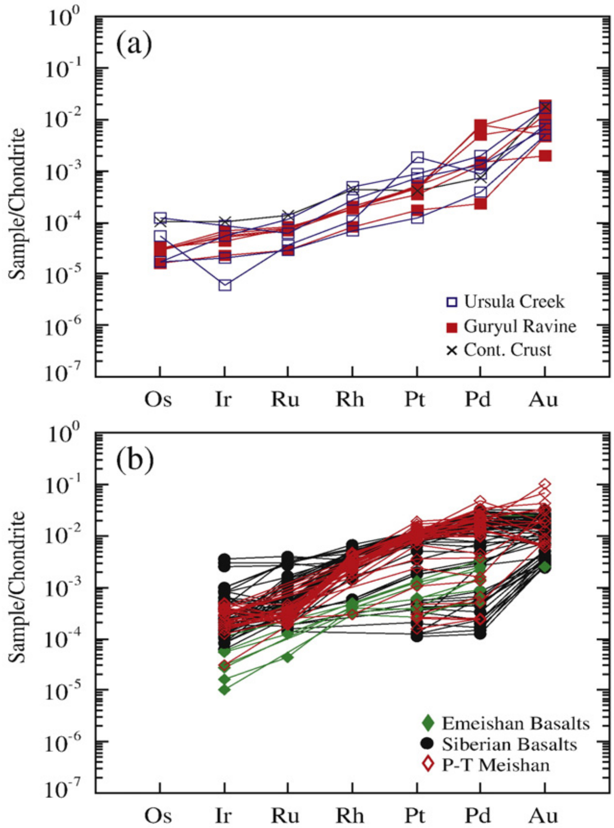

Fig. 5. Chondrite normalized plots of PGE for: a) Guryul (filled squares) and Ursula Creek (open squares) samples compared with average continental crust (Wedepohl, 1995); b) Emeishan and Siberian basalts, and Permo–Triassic boundary sediments at Meishan (Lightfoot and Keays, 2005; Song et al., 2006; Xu et al., 2007).

hand decreases from the base to the +0.75 m mark before increasing. Nickel, copper and zinc also show increases into the shales of the lowermost Khunamuh and Grayling Formations reaching a maximum at +0.4 m in both, though the Ursula Creek values are much less than at Guryul and drop back to low values by +1.2 m., whereas the higher values at Guryul tend to persist into the pyritic shales (Fig. 4). At Ursula Creek, anoxia is so far determined only by instrumentally-determined Th/U ratios which suggest anoxia began below the top of the Fantasque Formation below the level of the lowermost sample (UC 23) (Wignall and Twitchett, 2002).

At Guryul, the total organic carbon (TOC) stays between 0.2 and 0.5% in the relevant part of the Guryul section (Algeo et al., 2007), though this is metamorphosed to sub-greenschists facies (Brookfield et al., 2003), whereas the unmetamorphosed Ursula Creek section has TOC values in the relevant section of between 0.2 and 1.5% (Wang et al., 1994). The lack of correspondence of the PGE and TOC values suggest that the PGE are not associated with organic matter. The lack of correspondence of Ni, Cu, Zn and PGE values suggest that their concentrations are due to different processes, and that they are not detrital.

5. Comparison with other PGE-bearing rocks

PGE-bearing marine Permo–Triassic boundary horizons are increasingly being recognized around the world (Holser et al., 1989; Koeberl et al., 2004; Xu et al., 2007) with the highest values in the black shales that frequently mark the boundary (Table 3). Compared to Guryul and Ursula Creek, both Meishan and the Carnic Alps (Gartnerkofel, Val Bardia) have higher Ir values, but different Pd/Pt and Ir/Pt ratios and overall lower total PGE abundance. The maximum PGE are reached at +0.1 m (sample 26b) at Meishan; but in the Carnic Alps not only in the boundary black shale at Val Bardia (sample S0), but also in a black shale (sample 117S), 40 m above the paleontologically defined Permo–Triassic boundary at Gartnerkofel which suggests that the PGE values are not related to unique Permo–Triassic boundary conditions (Table 3). The PGE values in all these areas, as well as at Guryul and Ursula Creek are mostly not significantly above continental crustal values (Tables 2 and 3).

Unfortunately, little is known of PGE behaviour in sediments other than those at the *K–T* boundary and in some economically metalliferous black shales (Pasava, 1993; Lee et al., 2003). High PGE values are found in some thin horizons of metal-bearing marine black shales related to intracontinental rifts, either with or without contemporary basalts (Pasava, 1993) (Table 4, Kupferschiefer). High Pd/Pt ratios are, however, not only found in such marine black shales but also in volcanic gas condensates and some oceanic basalts, as well as from reducing continental margin sediments (Table 4).

The chondrite normalized PGE patterns for both Guryul and Ursula Creek are depleted in iridium–PGE and nearly parallel to equivalent strata at Meishan, the Emeishan basalts, Siberian Traps and Ontong Java plateau basalts (Fig. 5). The Guryul and Ursula Creek Ir/Pt (0.002–0.081) ratios are similar to those from Meishan, MORB, Emeishan basalts, Siberian basalts, Ontong Java Plateau, Kudrayev and reducing continental margin sediments (Fig. 6). The Pd/Pt versus Ir/Pt plots also show the Ursula Creek samples close to the origin and to values for the various basalts and sediments, and unlike any known extraterrestrial body (Bennett et al., 2000). The Pd/Pt plot for Guryul, however, shows very strong stratigraphically-controlled palladium enrichment to greater extent than the Ontong Java samples, and only matched by some Recent continental margin sediments and Kudrayev basalts (Fig. 6).

Table 3
PGE for Meishan (Xu et al., 2007) and Carnic Alps (Gartnerkofel, Val Bardia) (Koeberl et al., 2004).

	Meishan						Gartnerkofel			Val Bardia			
	24f	25a	25b	26a	26b	28	119	117S	116	SD 105	SD 55	S0	SU0–4
	0	0.005	0.01	0.05	0.1	0.3	185.96 m	185.57 m	185.51 m				
Ru (ng/g)	0.031			0.085			11.9	61.1	15.4	114.6	6	3.8	3.7
Rh (ng/g)	0.053	0.038	0.054	0.052	0.066	0.045							
Re (ng/g)							0.34	33.57	1.27	6.04	3.08	76.28	18.18
Pd (ng/g)	0.274	0.359	0.772	1.38	1.8	0.87		0.71					
Os (ng/g)							0.22	0.175	0.19	0.324	0.021	1.47	0.086
Ir (ng/g)	0.008	0.005	0.013	0.027	0.28	0.15	0.006	0.205	0.006			0.006	
Pt (ng/g)	0.372	0.256	0.577	1.03	1.3	0.375	0.03	36.1	0.08	0.23		0.27	
Au (ng/g)													
Pd/Pt	0.7	1.4	1.3	1.3	1.4	2.3		0.02					
Ir/Pt	0.02	0.02	0.02	0.03	0.2	0.4	2	5.7	750			22.2	
Rh/Ru	0.6			1.6									
Os/Ir							3.3	0.85	3.2			245	

Table 4
PGE for selected sediments and volcanics: Kupferschiefer, Poland (Bechtel et al., 2001), Fe/Mn crusts on Afanasiy–Nikitin seamount (Banakar et al., 2007); below Rainbow hydrothermal plume (Cave et al., 2003); Kudrayev volcano gas condensate (Distler et al., 2002); Ontong Java (Ely and Neal, 2003); recent continental margin reduced sediments from Gurvich (2006).

	Kupferschiefer, Poland			Afanasiy–Nikitin seamount	Rainbow plume	Kudrayev Volcano	Ontong Java plateau	Reducing sediments
	Oxidized Be 5	Transition Be 6	Reduced Be 7	Max value	Dr 25 av.	Gas condensate	Basalts	Continental margins
Os (ng/g)					0.1–0.5	60–400		0.15–0.46
Ir (ng/g)	14	67	48	14	0.02–0.4		0.4–1.3	0.01–0.70
Ru (ng/g)	38	24	36	31			0.2–2.2	
Rh (ng/g)	42	35	57	48			0.1–1.3	
Pt (ng/g)	413	574	11	780	0.5 –1.9	$0.5–0.8\times10^3$	4–27	0.7–3.5
Pd (ng/g)	465	536	43	4	0.1–2.0	$4–8\times10^3$	1.4–50.2	1.3–7.8
Au (ng/g)	32	141	5	2.5				
Re (ng/g)	118	206	948					
Pd/Pt	1.13	0.93	3.9	0.005	1–2	0.1–45	0.3–3.4	1.1–5.5
Ir/Pt	0.03	0.12	4.4	0.015	0.05–0.15		0.04–0.14	0.02–0.53
Rh/Ru	0.9	0.69	0.63	0.6			0.1–1.0	
Os/Ir					1.25–5.0			(0.6–3.5) and (1.2–5.5)

6. Discussion

The most significant point is that the PGE values in all previously analyzed Permo–Triassic sediments, as well as at Guryul and Ursula Creek are not significantly above continental crustal values. Though the significant clastic background sedimentation makes it difficult to compare values, the PGE ratios are incompatible with an extraterrestrial source (Alvarez et al., 1980; Koeberl et al., 2004) and unlike those of both nickel–iron and chondrite meteorites (Figs. 5 and 6) (Anders and Grevesse, 1989; Bennett et al., 2000; Horan et al., 2003).

The low PGE abundances and their ratios show that several possible explanations are unlikely. They did not accumulate over long periods of time during a hiatus in sedimentation. The PGE of condensed ferromanganese crusts now accumulating on existing sea floors are depleted in palladium — the opposite of Guryul and Ursula Creek (Banakar et al., 2007; Asavin et al., 2008) (Fig. 6, Table 4). As there is no significant PGE enrichment, they did not accumulate by hydrothermal precipitation (with other metals) in black shales related to intracontinental rifts as postulated for the Kupferschiefer and other PGE-rich black shales (Pasava, 1993)(Table 4).

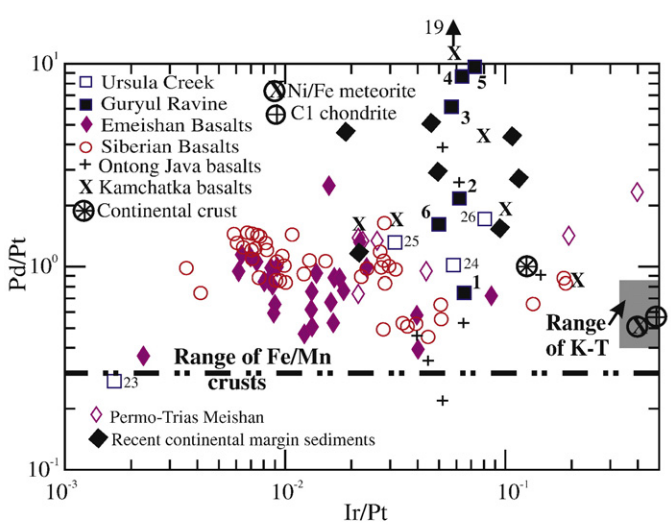

Fig. 6. Pd/Pt plotted against Ir/Pt for Guryul Ravine and Ursula Creek samples and compared with other terrestrial and extraterrestrial values (based on Xu et al., 2007, Fig. 4). Siberian basalts from Lightfoot and Keays (2005); Emeishan basalts from Song et al. (2006); average continental crust from Wedepohl (1995); Fe/Mn crusts and Fe meteorite from Banakar et al. (2007); Ontong Java Plateau basalts calculated from Ely and Neal (2003); Kamchatka Basalts from Ivanov et al. (2008); Recent continental margin reducing sediments from Ravizza and Pyle (1997).

The closest PGE concentrations and ratios to those of Guryul and Ursula Creek are those from the Cretaceous Ontong Java basalts, Kudrayev and reducing continental margin sediments (Pasava et al., 2007a; Sims et al., 2007) (Fig. 6; Table 4). A direct derivation of the Guryul PGE from such basalts, as in placer deposits (Orris and Bliss, 1985) and aerosols from degassing magmas observed in Hawaii and elsewhere (Distler et al., 2002), is unlikely given that possible sources are either very far away (Siberian Traps) or too old and covered with intervening sediments (Panjal Traps). At present, relatively rapid world-wide transportation of materials requires input into the stratosphere, either by explosive volcanic eruptions or by extraterrestrial impacts. But, though the Siberian Traps have significant thicknesses of pyroclastics (>400 m) at their base, these need not be caused by explosive, stratosphere-reaching eruptions but by phreatic eruptions (Ross et al., 2005). Basaltic eruptions, even those with abundant pyroclastics, are explosive only on a very small scale, and do not generate explosive Plinean phases. Even central-vent Strombolian lava jetting is of limited height (maximum 1200 m during a recent eruption of Etna, Sicily), so a far larger event or events are required to redistribute PGE from a single source to the world-wide extent seen at the *P–T* boundary. An alternative is that there was another large basaltic igneous province in the southern hemisphere of the same age as the Siberian Traps. Especially in view of the closeness of the Ontong Java Plateau, Kudrayev, and Guryul PGE ratios, and their difference from the Alpine and Meishan PGE ratios, a now-subducted end Permian oceanic basalt plateau is a plausible source and can be looked for in accreted complexes.

The PGE could have accumulated, however by: direct precipitation from seawater; by post-depositional migration during diagenesis, specifically caused by changes in redox potential (Colodner et al., 1992) and by differential take-up by organisms (Lee et al., 2003; Turner et al., 2007).

Direct precipitation from seawater fits the generally low, upper crustal values for the Guryul and Ursula creek PGE, and the Os/Ir ratios of major terrestrial, shallow marine reservoirs, and average Upper Continental Crust, which are close to 1.0 (Fig. 7), but not deep marine conditions where fractionation gives much higher Os/Ir ratios (Lee et al., 2003). The onset of anoxia in the latest Permian may have removed PGE to reduced sediments as has apparently been the case for many other black anoxic shales through time (Pasava, 1993). This is the preferred explanation of the PGE content of the black shales at the Permo–Triassic boundary — though post-depositional migration and fractionation, at least at Guryul, is likely given Guryul's low grade, water-rich chloritoid grade metamorphism (Brookfield et al., 2003), the different levels of Ni, Cu, and Zn enrichment and Pd enrichment, and the consistent increase in Pd/Pt ratios towards the lower limit of pyrite (Fig. 6). Limited post-depositional redistribution has been

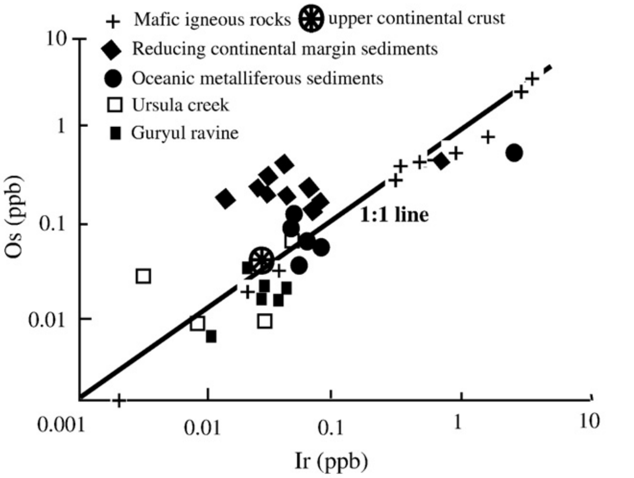

Fig. 7. Os versus Ir for selected mafic igneous rocks and sediments (from Ravizza and Pyle, 1997) plus Ursula creek and Guryul ravine samples.

found for the *K*–*T* boundary in oceanic sections (Lee et al., 2003) and for the epigenetic redox-controlled base-metal and PGE mineralization of the Kupferschiefer and other black shales (Pasava et al., 2003; Borg et al., 2005). PGE uptake by organisms, is known but has only recently been studied in any detail because of the importance of documenting anthropogenic input of PGE by catalytic converters (Hodge and Stallard, 1986). Furthermore, organometallic complexes can readily transport PGE both in groundwaters and volcanic fluids (Turner, 2006; Pasava et al., 2007b; Distler et al., 2008). Though not enough is currently known to evaluate organic uptake, in view of the low TOC of both sections and the lack of relationships between TOC and PGE, we consider organic uptake an unlikely explanation.

7. Conclusions

Analysis of latest Permian horizons in Kashmir and British Columbia show slightly elevated values of PGEs whose character indicate terrestrial sources, as has been found in China and Europe (Koeberl et al., 2004; Xu et al., 2007). The sources, however, need not be the same, since the PGE ratios differ from one area to another and the most values are not much different from those of average Upper Continental Crust (Table 2). The PGE content in the ubiquitous black shales that, in most places, directly follow the LPEH suggest that anoxia in the latest Permian may be the primary cause of the (generally small) increase in PGE (Colodner et al., 1992), though the resulting geochemistry of the sediments may also have contributed to post-deposition migration and precipitation. Thus, the PGE contents at the Permo–Triassic boundary in Guryul, Ursula Creek, and elsewhere, as well as those of other Phanerozoic metalliferous black shale horizons (Bechtel et al., 2001; Coveney, 2003; Pasava et al., 2003), are themselves controlled by the geological settings and depositional environments developed at that time. The PGE characteristics of the Guryul and Ursula Creek samples reflect the character of their sources and syn- and post-depositional concentration and fractionation of the PGE elements by a number of hydrous processes involving seawater, oxidation–reduction, and pH changes. The PGE characteristics of these sections cannot be attributed to any significant contribution from any extraterrestrial body.

However, much further work is required; first to investigate and explain the PGE characteristics of modern sediments, and second to characterize in greater detail (down to cm level) the various physical, chemical and biological changes across the *P*–*T* boundary world-wide and infer their causes. This is in progress for Guryul.

Acknowledgements

We thank Ms. Sumita Koul and other graduate students from Jammu University for help in collecting samples in Kashmir. Both MEB and JGS acknowledge generous financial and other support from the Institute of Earth Sciences, Academia Sinica, Taiwan (via the Director, Bor-Ming Jahn) and from the Postgraduate Department of Earth Sciences, Jammu University, India (via Dr. Ghulam Bhat). Qi Liang is supported by "CAS Hundred Talents" Project from Chinese Academy of Sciences. We appreciate the careful and constructive reviews of earlier drafts of the manuscript by Chris Koeberl and Tom Algeo.

References

Algeo, T., Hannigan, R., Rowe, H., Brookfield, M.E., Baud, A., Krystyn, L., Ellwood, B., 2007. Sequencing events across the Permian–Triassic boundary, Guryul ravine (Kashmir, India). Palaeogeography, Palaeoclimatology, Palaeoecology 252, 328–346.

Alvarez, L.W., Alvarez, W., Asaro, F., Michel, H.V., 1980. Extraterrestrial cause for the Cretaceous–Tertiary extinction. Science 208, 1095–1108.

Anders, E., Grevesse, N., 1989. Abundances of the elements: meteoritic and solar. Geochimica et Cosmochimica Acta 53, 197–214.

Asavin, A.M., Anikeeva, L.I., Kazakova, V.A., Andrreeev, S.I., Sapozhnikov, D.A., Roshchina, I.A., Kogarko, L.N., 2008. Trace element and PGE distribution in layered ferromanganese crusts. Geochemistry International 46, 1179–1205.

Banakar, V.K., Hein, J.R., Rajani, R.P., Chodankar, A.R., 2007. Platinum group elements and gold in ferromanganese crusts from Afanasiy–Nikitin seamount, equatorial Indian Ocean: sources and fractionation. Journal of Earth Systems Science 116, 3–13.

Bechtel, A., Ghazi, A.M., Elliot, W.C., Oszczepalski, S., 2001. The occurrences of the rare earth elements and the platinum group elements in relation to base metal zoning in the vicinity of Rote Fäule in the Kupferschiefer of Poland. Applied Geochemistry 16, 375–386.

Bennett, V.C., Norman, M.D., Garcia, M.O., 2000. Rhenium and platinum element abundances correlated with mantle source components in Hawaiian picrites: sulphides in the plume. Earth and Planetary Science Letters 183, 513–526.

Borg, G., Frotzscher, M., Ehling, B., 2005. Metal content and spatial distribution of Au and PGE in the Kupferschiefer of the Mansfield/Sangerhausen mining district, Germany. In: Jingwen Mao, Bierlen, F.P. (Eds.), Mineral Deposit Research: Meeting the Global Challenge, Volume 2. Springer Verlag, Berlin, pp. 885–888.

Brookfield, M.E., 1993. The Himalayan passive margin from Precambrian to Cretaceous times. Sedimentary Geology 84, 1–35.

Brookfield, M.E., Twitchett, R.J., Goodings, C., 2003. Palaeoenvironments of the Permian–Triassic transition sections in Kashmir, India. Palaeogeography, Palaeoclimatology, Palaeoecology 198, 353–371.

Brookfield, M.E., Blechschmidt, I., Hannigan, R., Coniglio, M., Simonson, B., Wilson, G., 2006. Sedimentology and geochemistry of extensive very coarse deepwater fan sediments in the Middle Jurassic of Oman, emplaced by giant tsunami triggered by submarine mass flows. Sedimentary Geology 192, 75–98.

Cave, R.R., Ravizza, G.E., German, C.R., Thomson, J., Nesbitt, R.W., 2003. Deposition of osmium and other platinum-group elements beneath the ultramafic-hosted Rainbow hydrothermal plume. Earth and Planetary Science Letters 210, 65–79.

Colodner, D.C., Boyles, E.A., Edmond, J.M., Thompson, J., 1992. Post-depositional mobility of platinum, iridium, and rhenium in marine sediments. Nature 358, 402–404.

Coveney Jr., R.M., 2003. Metalliferous Paleozoic black shales and associated strata. In: Lentz, D.R. (Ed.), Geochemistry of Sediments and Sedimentary Rocks: Evolutionary Considerations to Mineral Deposit-forming Environments. Geological Association of Canada, St John's, Newfoundland, pp. 135–144.

Distler, V., Yudovskaya, M., Chaplygin, I., Znamensky, V., 2002. PGE in the modern hydrotherms of Kudrayavy Volcano (Kuril Islands). The International Platinum Symposium, Billings, Montana: Extended Abstracts. 4 pp.

Distler, V., Dikov, Yu.P., Yudovskaya, M.A., Chaplygin, I.V., Buleev, M.I., 2008. Platinum–chlorine–phosphorous–hydrocarbon complex in volcanic fluids: the first find in the terrestrial environment. Doklady Earth Sciences 420, 628–631.

Ely, J.C., Neal, C.R., 2003. Using platinum-group elements to investigate the origin of the Ontong Java Plateau, SW Pacific. Chemical Geology 196, 235–257.

Erwin, D.H., 2005. Extinction: How Life on Earth Nearly Died 250 Million Years Ago. Princeton University Press, Princeton. 306 pp.

Govindaraju, K., 1994. Complication of working values and sample description for 383 geostandards. Geostandards and Geoanalytical Research 18, 1–158.

Henderson, C.M., Mei, S., 2000. Preliminary cool-water Permian conodont zonation in North Pangea: a review. Permophiles 36, 16–23.

Hodge, V.F., Stallard, M.O., 1986. Platinum and palladium in roadside dust. Environmental Science and Technology 20, 1058–1060.

Holser, W.T., et al., 1989. A unique geochemical record at the Permian/Triassic boundary. Nature 337, 39–43.

Horan, M.F., Walker, R.J., Morgan, J.W., Grossman, J.N., Rubin, A.E., 2003. Highly siderophile elements in chondrites. Chemical Geology 196, 5–20.

IUPAC (International union of pure and applied chemistry), 1991. Isotopic compositions of the elements 1989. Pure and Applied Chemistry 63, 991–1002.

Ivanov, A.V., Perepelov, A.B., Palesskii, S.V., Nikolaeva, I.V., 2008. First data on the distribution of platinum group elements (Ir, Os, Ru, Pt, and Pd) and Re in island-arc basalts of Kamchatka. Doklady Earth Sciences 420, 507–601.

Jones, D.L., 1990. Synopsis of late Paleozoic and Mesozoic terrane accretion within the Cordillera of western North America. Philosophical Transactions of the Royal Society of London A331, 479–486.

Kaiho, K., Chen, Z.-Q., Kawahata, H., Kajiwara, Y., Sato, H., 2006. Close-up of the end Permian mass extinction horizon recorded in the Meishan section, South China: sedimentary, elemental, and biotic characterization and a negative shift of sulfur isotope ratio. Palaeogeography, Palaeoclimatology, Palaeoecology 239, 396–405.

Koeberl, C., Farley, K.A., Peucker-Ehrenbrink, B., Sephton, M.A., 2004. Geochemistry of the end-Permian extinction event in Austria and Italy: no evidence for an extraterrestrial component. Geology 32, 1053–1056.

Lee, C.-T.A., Wasserburg, G.J., Kyte, F.T., 2003. Platinum-group elements (PGE) and rhenium in marine sediments across the Cretaceous–Tertiary boundary: constraints on Re-PGE transport in the marine environment. Geochimica et Cosmochimica Acta 67, 655–670.

Lightfoot, P.C., Keays, R.R., 2005. Siderophile and chalcophile metal variations in flood basalts from the Siberian trap, Noril'sk region: implications for the origin of the Ni–Cu–PGE sulfide ores. Economic Geology 100, 439–462.

Meisel, T., Moser, J., 2004. Reference materials for geochemical PGE analysis: new analytical data for Ru, Rh, Pd, Os, Ir, Pt and Re by isotope dilution ICP-MS in 11 geological reference materials. Chemical Geology 208, 319–338.

Murchey, B.L., Jones, D.L., 1992. A mid-Permian chert event: widespread deposition of biogenic siliceous sediments in coastal island arc and oceanic basins. Palaeogeography, Palaeoclimatology, Palaeoecology 96, 161–174.

Nakazawa, K., Kapoor, H.M., Ishii, K., Bando, Yi., Okimura, Y., Tokuoka, T., 1975. The Upper Permian and Lower Triassic in Kashmir, India. Memoirs of the Faculty of Science, Kyoto University, Series Geology and Mineralogy 42, 1–106.

Orris, G.J., Bliss, J.D., 1985. Geologic and grade-volume data on 330 gold placer deposits. U.S. Geological Survey Open-File Report 85, 172 pp.

Pasava, J., 1993. Anoxic sediments — an important environment for PGE; an overview. Ore Geology Review 8, 425–445.

Pasava, J., Barnes, S.-H., Vymazalova, A., 2003. The use of mantle normalization and metal ratios in the identification of the sources of platinum-group elements in various metal-rich black shales. Mineralium Deposita 38, 775–783.

Pasava, J., Vymazalova, A., Petersen, S., 2007a. PGE fractionation in seafloor hydrothermal systems: examples from mafic- and ultramafic-hosted hydrothermal fields at the slow-spreading Mid-Atlantic Ridge. Mineralium Deposita 42, 423–431.

Pasava, J., Sklodowska, A., Vymazalova, A., Biernat, A., Kribek, B., Orberger, B., 2007b. Organometallic complexes from Ni–Mo–PGE black shales in South China — combination of bioactivities, hydrothermal venting and phosphate deposition during global Cambrian biological explosion. Goldschmidt Conference Abstracts 2007, A763.

Qi, L., Zhou, M.F., 2008. Determination of platinum-group elements in OPY-1: comparison of results using different digestion techniques. Geostandards and Geoanalytical Research 32, 377–387.

Qi, L., Zhou, M.F., Wang, C.Y., 2004. Determination of low concentrations of platinum group elements in geological samples by ID-ICP-MS. Journal of Analytical Atomic Spectrometry 19, 1335–1339.

Qi, L., Zhou, M.F., Wang, C.Y., Sun, M., 2007. Evaluation of a technique for determining Re and PGEs in geological samples by ICP-MS coupled with a modified Carius tube digestion. Geochemical Journal 41, 407–414.

Ravizza, G., Pyle, D., 1997. PGE and Os isotopic analyses of single sample aliquots with NiS fire assay preconcentration. Chemical Geology 141, 251–268.

Ross, P.-S., Peate, I.U., McClintock, M.K., Xu, Y.G., Skilling, I.P., White, J.D.L., Houghton, B.F., 2005. Mafic volcaniclastic deposits in flood basalt provinces: a review. Journal of Volcanology and Geothermal Research 145, 281–314.

Rudnik, R.L., Gao, S., 2005. Composition of the continental crust. In: Rudnik, R.L. (Ed.), Treatise on Geochemistry 3: the Crust. Elsevier, Amsterdam, pp. 1–64.

Sheng, Jinshang, Chen, Chuzhen, Wang, Yigang, Rui, Lin, Liao, Zhuoting, Dando, Y., Ishii, K., Nakazawa, K., Nakamura, K., 1984. Permian–Triassic boundary in middle and eastern Tethys. Journal of Faculty of Sciences, Hokkaido University, Ser IV 21 (1), 133–181.

Sims, K.W.W., Peucker-Ehrenbrink, B., Mather, T., Pyle, D., Martin, R.S., Gauthier, R.P.-J., Aiuppa, A., 2007. Sniffing for clues to the dinosaurs demise: measurements of osmium isotopes composition and platinum group element abundances in volcanic emissions. International Conference on evolution, transfer and release of magmas and volcanic gases, Taipei, Taiwan, 22–27 April, 2007. Preliminary Abstract Volume, p. 41.

Song, X.Y., Zhou, M.F., Keays, R.R., Cao, Z.M., Sun, M., Qi, L., 2006. Geochemistry of the Emeishan flood basalts at Yangliuping, Sichuan, SW China: implications for sulfide segregation. Contributions to Mineralogy and Petrology 152, 53–74.

Turner, A., 2006. Enzymatic-availability of trace metals in estuarine sediment. Marine Chemistry 98, 140–147.

Turner, A., Lewis, M., Shams, L., Brown, M., 2007. Uptake of platinum group elements by the marine macroalga, *Ulva lactuc*a. Marine Chemistry 105, 271–280.

Wang, K., Geldsetzer, H.H.J., Krouse, H.R., 1994. Permian–Triassic extinction: organic δ^{13}C evidence from British Columbia, Canada. Geology 22, 580–584.

Wedepohl, K.H., 1995. The composition of the continental crust. Geochimica et Cosmochimica Acta 59, 1217–1232.

Wignall, P.B., Newton, R., 2003. Contrasting deep-water records from the Upper Permian and Lower Triassic of South Tibet and British Columbia: evidence for a diachronous mass extinction. Palaios 18, 153–167.

Wignall, P.B., Twitchett, R.J., 2002. Extent, duration and nature of the Permian–Triassic superanoxic event. In: Koeberl, C., Macleod, K.G. (Eds.), Catastrophic Events and Mass Extinction: Impacts and Beyond: Geological Society of America Special Paper, vol. 356, pp. 395–413.

Wignall, P.B., Newton, R., Brookfield, M.E., 2005. Pyrite framboid evidence for oxygen-poor deposition during the Permian–Triassic crisis in Kashmir. Palaeogeography, Palaeoclimatology, Palaeoecology 216, 183–188.

Xu, D.-Y., Yan, Z., 1993. Carbon isotope and iridium event markers near the Permian/Triassic boundary in the Meishan section, Zhejiang Province, China. Palaeogeography, Palaeoclimatology, Palaeoecology 104, 171–176.

Xu, L., Lin, Y., Shen, W., Qi, L., Xie, L., Ouyang, Z., 2007. Platinum-group elements of the Meishan Permian–Triassic boundary section: evidence for flood basaltic volcanism. Chemical Geology 246, 55–64.

Yin, H., Kexin, Z., Jinnan, T., Zunyi, Y., Shunbao, W., 2001. The Global Stratotype Section and Point (GSSP) of the Permian–Triassic Boundary. Episodes 24, 102–114.